

A Near Infrared Spectroscopic Survey of LINER Galaxies

J. E. LARKIN

Dept. of Astronomy and Astrophysics, University of Chicago and
Palomar Observatory, California Institute of Technology

L. ARMUS, R. A. KNOP, B. T. SOIFER & K. MATTHEWS
Palomar Observatory, California Institute of Technology

ABSTRACT

This paper reports the results of a near infrared spectroscopic survey of LINER galaxies undertaken with a new infrared spectrograph at the 5 m Hale telescope. The galaxy sample includes 11 LINERs with spectra covering the [FeII] (1.2567 μm), Pa β (1.2818 μm), H₂ (1-0 S(1), 2.1218 μm) and Br γ (2.1655 μm) near infrared emission lines, and one additional galaxy with only [FeII] and Pa β line coverage.

All of the LINERs with infrared line detections have strong [FeII] and/or H₂ emission, with about half (4 out of 9) having extremely high ratios (>2) of [FeII] to Pa β . The strength of the H₂ and [FeII] lines is well correlated with the optical [OI] line, with many LINERs having higher ratios of [FeII]/Pa β , H₂/Br γ and [OI]/H α than other galaxy types. The LINERs with the highest [FeII]/Pa β ratios (termed “strong” [FeII] LINERs) show evidence for recent star formation. Shocks from compact supernova remnants may enhance the [FeII] emission in these “strong” [FeII] LINERs. The LINERs with lower [FeII]/Pa β ratios (termed “weak” [FeII] LINERs) are more consistent with Seyfert-like activity, including higher ionization states, some strong x-ray sources and some broad H α detections. The [FeII] luminosity and the [FeII]/Pa β ratio in these objects are more easily explained by hard x-ray excitation than in the “strong” [FeII] LINERs. These “weak” [FeII] LINERs are considered prime candidates for being low luminosity Seyfert nuclei.

1. Introduction

LINERs (Low Ionization Nuclear Emission-line Region galaxies) are the most common and lowest energy examples of active galaxies known (Heckman 1980). The main LINER

characteristic is unusually strong forbidden line transitions from low ionization states such as [OII]($\lambda=3727 \text{ \AA}$), [NII]($\lambda=6583 \text{ \AA}$), and [SII]($\lambda=6717,6731$) relative to lines from higher ionization states. The original definition used by Heckman (1980) was [OII]($\lambda=3727 \text{ \AA}$) / [OIII]($\lambda=5007 \text{ \AA}$) > 1 and [OI]($\lambda=6300 \text{ \AA}$) / [OIII]($\lambda=5007 \text{ \AA}$) $> 1/3$. Classical LINER galaxies also have much less total energy in the spectral lines as compared to Seyfert galaxies and other types of active galactic nuclei (AGN); often down by a factor of a 100 in comparison to Seyfert’s. The weakness of the spectral lines makes LINERs difficult to study, particularly when the galaxies often have strong stellar absorption features.

Fast ($v \sim 100 \text{ km s}^{-1}$) shocks (Heckman, 1980), photoionization from a power-law source (e.g. Ho, Filippenko, & Sargent 1993) or from a cluster of very hot stars (e.g. Terlevich & Melnick 1985; Shields 1992), especially in very dense environments, can all duplicate the observed emission line flux ratios in LINERs. An important aspect of the star formation models, involves compact supernova remnants which are confined by the high densities within the nuclear region and which produce strong shocks. X-ray heating is particularly attractive for photoionization because hard x-rays are able to penetrate deeply into molecular clouds creating large partially ionized regions where low ionization species will dominate.

An intriguing possible variation on the photoionization models recently proposed by Eracleous, Livio & Binette (1995), is that LINERs have a compact object (probably a black hole) in the nucleus which periodically disrupts a star during a close orbital approach. As the stellar material accretes onto the central source, high energy photons are produced and a Seyfert-like broad line region appears. As the material is consumed, the ionizing flux drops and the high ionization states weaken quickly. Low ionization lines, however, remain strong for much longer since the decay time is longer and the light crossing time in this region is much larger than that of the broad line region. This “Duty Cycle Hypothesis” was motivated by the observation that about 20% of LINERs had detectable 2300 \AA emission with HST (Maoz et al. 1995). These UV bright galaxies, have no other obvious difference from the UV dark LINERs. Under this theory, the UV bright galaxies would still have ongoing accretion, while the others are in the quiescent phase. In support of this theory, Eracleous et al. (1995) point to NGC 1097 which was observed to make a sudden transition from a LINER to a Seyfert 1 (Storchi-Bergmann, Baldwin & Wilson 1993).

It is also possible that LINERs represent a heterogeneous class of objects. Some LINERs may have a central “monster” like Seyfert galaxies, while others have one or more dense clusters of hot young stars. Shocks may play a role in enhancing the forbidden lines in either of these two groups. Whatever the case, extending the number of observed spectral

diagnostics into the infrared gives greater leverage on the problem of understanding the ultimate origin of the LINER phenomena.

A significant number of important infrared spectral features exist which can provide useful astrophysical insights. Among these are the $\text{Br}\gamma$ ($2.1655\mu\text{m}$) and $\text{Pa}\beta$ ($1.2818\mu\text{m}$) hydrogen recombination lines. These lines trace ionizing photons and can be directly related to other recombination lines and to the strength of the UV continuum, while suffering much less from dust extinction than the Balmer lines. Another series of important infrared lines are the H_2 rotation-vibration transitions which have no analog within the optical. The strongest H_2 line is the 1-0 S(1) transition at $2.1218\mu\text{m}$. H_2 emission is ubiquitous in starburst and Seyfert galaxies and is thought to originate in slow shocks, UV fluorescence and X-ray heating. The forbidden transitions of singly ionized iron ([FeII]), are also strong in the infrared. Iron is believed to play an important role as a coolant in shocked environments (Nussbaumer and Storey 1988) but in the general interstellar medium it is often depleted compared to other elements since most iron is locked up in dust grains. The strongest near infrared [FeII] line is the $1.2567\mu\text{m}$ transition in the J band. This line is often very strong in Seyfert galaxies and in most cases is thought to trace faster shocks ($\sim 100\text{ km sec}^{-1}$) than the H_2 lines (Graham et al. 1990). [FeII] is also thought to be strong in x-ray heated environments where dust grains have been evaporated.

In this paper, we report new near infrared spectroscopy of a sample of bright LINERs, and we attempt to use these data to constrain the possible excitation mechanisms.

2. Observing Procedures and Data Reductions

2.1. Target Selection and Observing Strategy

The target list began with the original sample of 30 LINERs (including several “transition” objects which have line ratios on the border between LINERs and Seyferts) from Heckman (1980), which are in the right ascension range between $8^{\text{h}}30^{\text{m}}$ and $13^{\text{h}}30^{\text{m}}$. To extend the target list, additional galaxies were selected from Keel (1983) and Ho et al. (1993). Because of bad weather during most of the spring runs, half of the objects observed with the infrared spectrograph are from these additional surveys. In the end 11 classical LINERs were observed in both the J and K bands and 1 additional galaxy had only J-band spectra taken. Table 1 lists the galaxies observed, the dates of the observations, and the wavelengths covered.

TABLE 1
Near Infrared Spectroscopy Observing Log

Object (1)	RA(1950) (2)	Dec(1950) (3)	cz (km s^{-1}) (4)	Date (5)	Central λ (6)	Res. ($\frac{\lambda}{\Delta\lambda}$) (7)	P.A. (deg) (8)
NGC 0404	01h06m39.3s	+35d27m10s	-43	94/08/19	1.2567	1000	128
					2.1470	820	128
NGC 2685	08h51m40.7s	+58d55m33s	877	95/03/14	1.2683	1020	305
					2.1860	815	305
NGC 3992	11h55m00.8s	+53d39m11s	1051	94/05/22	1.2707	1020	270
					2.1532	800	270
NGC 3998	11h55m20.9s	+55d43m56s	1138	95/05/13	1.2671	1020	270
					2.1762	810	270
NGC 4258	12h16m29.8s	+47d34m51s	449	94/05/22	1.2707	1020	58
					2.1532	800	58
NGC 4589	12h35m29.0s	+74d27m59s	1825	95/03/14	1.2683	1020	343
					2.1501	800	343
NGC 4736	12h48m31.9s	+41d23m32s	307	95/03/12	1.2683	1020	35
					2.1801	820	35
NGC 4826	12h54m16.9s	+21d57m18s	350	95/03/13	1.2683	1020	270
					2.1801	820	270
NGC 5194	13h27m46.0s	+47d27m22s	467	94/05/23	1.2707	1020	170
					2.1532	800	170
				94/07/26	1.2837	1020	170
NGC 7217	22h05m37.9s	+31d06m52s	1400	94/07/26	2.1649	810	170
					1.2679	1020	270
NGC 7479	23h02m26.41s	+12d03m11s	2800	94/08/21	1.2837	1060	55
					2.1649	810	55
NGC 7743	23h41m48.6s	+9d39m25s	1710	94/07/27	1.2693	1020	270
					2.1515	780	270

Since LINERs typically have faint emission features, it is important to concentrate the observations on the potentially brightest near infrared lines. Among those lines accessible at zero redshift, $\text{Pa}\beta$ is typically the brightest feature in AGN and starburst galaxies. Under case B recombination, $\text{Br}\gamma$ is fainter than $\text{Pa}\beta$ by a factor of about six, but is still usually one of the brightest lines. The brightest Fe^+ line is at $1.2567 \mu\text{m}$ which is only $0.0251 \mu\text{m}$ away from $\text{Pa}\beta$, making this an obvious pair of lines to observe simultaneously. The strongest H_2 line available at zero redshift is from the 1-0 S(1) transition at $2.1218 \mu\text{m}$. This line is separated by $0.0437 \mu\text{m}$ from $\text{Br}\gamma$, again creating an obvious pair of lines to observe simultaneously. In order to maximize the number of LINERs observed, only these two settings were observed.

2.2. Near Infrared Spectroscopy at the 200 Inch Hale Telescope

Near infrared spectra were obtained using the 200 inch Hale telescope at Palomar Observatory from 1994 April to 1995 May. The spectra were taken with a new near infrared longslit spectrometer, described in Larkin et al. (1996). For all observations, the lower resolution grating ($R \sim 1000$) was used with the slit set at $0.75'' \times 40''$. To center the objects on the slit, images were first taken through a wide open slit ($10'' \times 40''$) and the telescope was moved to place the nuclear centroid onto the slit center. The position angle of the slit was selected either by aligning the slit along a position angle of known extended $\text{H}\alpha$ emission (Larkin et al. 1997, in preparation) or by orienting the slit along the minor axis. For all objects the galaxy was moved back and forth along the slit between two locations $10''$ from the opposite ends of the slit ($20''$ between the two positions). In this way, each spectrum in a pair could serve as the sky frame for image subtraction of the other mated spectrum. Two grating angles were typically used to give rest frame wavelength coverages from 1.245 to $1.300 \mu\text{m}$ ($R \sim 1050$), and 2.087 to $2.207 \mu\text{m}$ ($R \sim 850$). These wavelength ranges were selected to include the redshifted $[\text{FeII}]$ ($\lambda = 1.2567 \mu\text{m}$), and $\text{Pa}\beta$ ($\lambda = 1.2818 \mu\text{m}$) spectral lines, and the redshifted H_2 ($\lambda = 2.1218 \mu\text{m}$) and $\text{Br}\gamma$ ($\lambda = 2.1655 \mu\text{m}$) lines. All wavelengths quoted in this paper are values in air.

The Yale Bright Star Catalog (Hoffleit 1964) was used to select main sequence G stars that were observed close in time and airmass to the galaxies in order to remove telluric absorption from the galaxy spectra and to serve as flat fields. The chopping secondary of the telescope was driven with a triangular waveform to move the star back and forth along the slit to uniformly illuminate the array. The stars represent a good approximation to an ideal blackbody at these wavelengths except for weak hydrogen absorption lines. In order

to properly correct the galactic spectra, these lines must first be removed from the stellar spectra by interpolation. For all of the galaxies in the sample except NGC 404, the redshift is high enough ($>300 \text{ km s}^{-1}$) that contamination from the interpolated portion of the G star spectra should not affect the emission lines observed.

The galaxy spectra were reduced by first subtracting image pairs. The galaxy frames were then divided by the interpolated star frames. Bad pixels were then replaced by the median of their neighboring pixels. Atmospheric OH emission lines in the stellar spectrum were fit with third order polynomials in order to remove a slight curvature in the spectral lines and to wavelength calibrate the spectra. Wavelengths for the OH lines were obtained from Oliva and Origlia (1992). Slight spatial curvature was removed by fitting spectra taken of a calibrator star which was moved in $5''$ steps along the slit.

2.3. Near Infrared Imaging at the 200 Inch Hale Telescope

Broad band $1.25\mu\text{m}$ (J-band) and $2.2\mu\text{m}$ (K-band) images taken with a mirror placed in front of the grating were used to flux calibrate the spectra. These images, were themselves flux calibrated by matching synthetic aperture fluxes in the images with aperture photometry from either Neugebauer et al. (1987), Aaronson (1977), or Willner et al. (1985). A $0.75'' \times 3''$ synthetic aperture on the same broad band images was then used to determine the flux densities within the slit for the spectroscopic observations. These “slit” measurements were then used to scale the counts in the spectra to actual flux.

3. Results

The flux calibrated spectra for the 12 classical LINERs observed at ~ 1000 resolution are shown in figure 1. The J-band spectra are shown in the left panel and the K-band in the right. Many of the spectra have been shifted upwards to prevent overlap and the amount of the shift is indicated in parenthesis next to the galaxy’s name. The locations of the most common emission and absorption features are marked at the top of each panel. The [FeII] line at $1.2567\mu\text{m}$ is the most common emission line detected, being present in 8 of the 12 galaxies. The H_2 line at $2.1218\mu\text{m}$ is also a common feature, being found in 4 of the 11 galaxies with K-Band spectra. $\text{Pa}\beta$ ($1.2818\mu\text{m}$), which is typically the strongest near infrared line available at zero redshift, is only found in emission in 2 galaxies, NGC 5194

and NGC 7479. $\text{Br}\gamma$ ($2.166\mu\text{m}$) is undetected in all 11 galaxies with K-Band spectra (note some of the spectra show features near $\text{Br}\gamma$ due to residual hydrogen absorption features in the calibration stars). Detection limits varied between the objects but lines as faint as 1.0×10^{-15} ergs $\text{s}^{-1} \text{cm}^{-2}$ were detected in some galaxies. Table 2 gives the measured fluxes and uncertainties for the infrared lines. In most cases a $3''$ by 1000 km s^{-1} aperture was placed on the continuum subtracted spectra to determine the fluxes making the true aperture on the sky $3''$ by $0.75''$ (the slit width). The uncertainties were determined by placing the same aperture at several locations on the spectra above and below each emission line. In many cases, $\text{Pa}\beta$ is detected in absorption, and the strength is listed as a negative value in the table. Table 2 also gives the equivalent widths of the $[\text{FeII}]$ and H_2 lines in columns 6 and 7. In all cases, the emission lines were not resolved spatially with seeing of ~ 1.0 arcsec.

TABLE 2
Measured Line Fluxes and Equivalent widths

Object (1)	flux ($\times 10^{-15}$ erg $\text{cm}^{-2} \text{s}^{-1}$)				EqW. (\AA)	
	$[\text{FeII}]$ (2)	$\text{Pa}\beta$ (3)	H_2 (4)	$\text{Br}\gamma$ (5)	EqW($[\text{FeII}]$) (6)	EqW(H_2) (7)
NGC 0404	7.8 ± 0.2	-1.3 ± 0.3	2.4 ± 0.7	0 ± 1^b	3.1 ± 0.3	3.1 ± 0.3
NGC 2685	0 ± 1	-1.5 ± 1	0 ± 1	0 ± 1	< 0.5	< 2
NGC 3992	0 ± 1	-2 ± 1	0 ± 0.5	0 ± 0.5	< 0.7	< 1
NGC 3998	3.1 ± 0.7	-1 ± 1	0 ± 1	0 ± 1	1.7 ± 0.2	< 1
NGC 4258	3.5 ± 0.6	-0.4 ± 0.6	0 ± 0.9	0 ± 0.9	1.5 ± 0.2	< 1
NGC 4589	0 ± 2	-2.6 ± 2	0 ± 0.8	0 ± 0.8	< 1	< 1
NGC 4736	10 ± 4	-8 ± 3	0 ± 2	0 ± 4	0.8 ± 0.4	< 0.5
NGC 4826	4 ± 2	-2.6 ± 2	0 ± 0.5	0 ± 2	0.9 ± 0.4	< 0.3
NGC 5194 ^a	5.8 ± 0.9	1.0 ± 0.7	3.9 ± 0.6	0 ± 1	2.8 ± 0.4	5.6 ± 0.8
	7.8 ± 0.9	1.5 ± 0.4	4.7 ± 0.7	0.5 ± 0.3	3.7 ± 0.5	7 ± 1
NGC 7217	2.3 ± 0.7	-1.5 ± 0.7	-	-	1.4 ± 0.4	-
NGC 7479	0 ± 0.3	1.3 ± 0.4	2.8 ± 0.6	0 ± 0.6^b	< 0.5	9 ± 2
NGC 7743	4.5 ± 1	-1.2 ± 1	3.7 ± 0.4	0 ± 0.5	2.8 ± 0.6	4.6 ± 0.6

^a NGC 5194 was observed twice, the May 94 values are given above the July 94 values.

^b Although a small bump or wiggle appears near $\text{Br}\gamma$ in these galaxies, it is probably noise or residual from the calibration star.

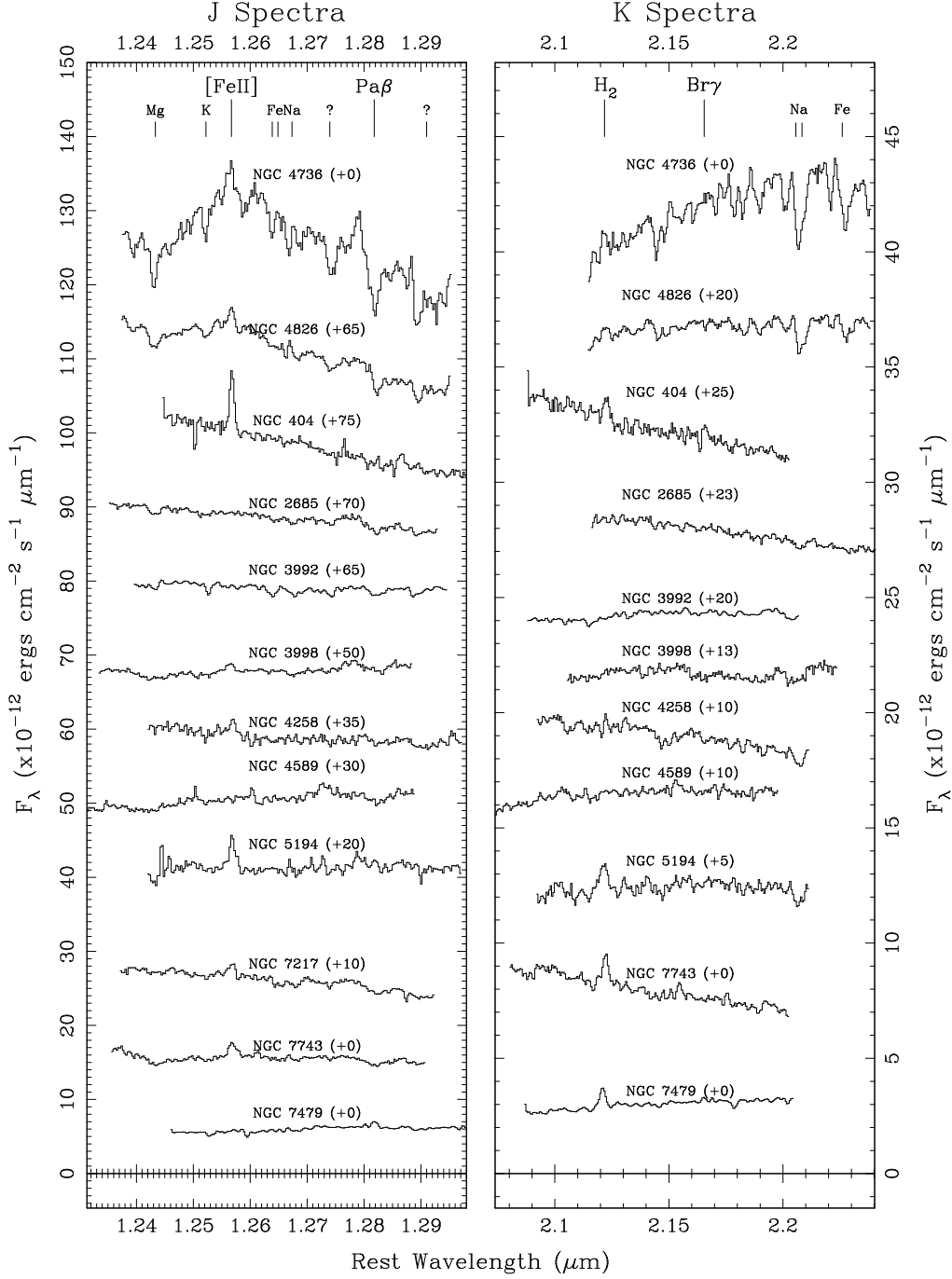


Fig. 1.— Flux calibrated spectra of individual galaxies: The left spectra are in the J-band window and include the wavelengths of [FeII] ($\lambda_{rest}=1.2567\mu\text{m}$) and Pa β at a resolution of ~ 1050 . The right spectra are in the K-band window and include the wavelengths of H₂ ($\lambda_{rest}=2.1218\mu\text{m}$) and Br γ at a resolution of ~ 850 . The spectra of each galaxy have been shifted up by a constant amount to prevent the spectra from overlapping. The amount shifted up is in units of 10^{-12} ergs cm^{-2} s^{-1} μm^{-1} and is given in parenthesis next to each galaxies name. The spectra have also been shifted in wavelength to the galaxy’s restframe. The locations of emission lines and atomic absorption features are also marked at the top of each graph. The emission lines are given in larger type and are marked higher than the atomic lines.

3.1. Estimated Pa β and Br γ strengths

Even though Pa β and Br γ are usually not detected in emission, it is important to try and estimate their strengths because these lines are directly proportional to the ionizing photon flux, and provide useful reddening insensitive ratios with the [FeII] and H $_2$ lines, respectively. We use an extrapolation from the optical recombination lines to estimate the infrared recombination line emission strengths. This technique uses the case B recombination ratios for hydrogen (Osterbrock 1989). Differential reddening between H α and Pa β was removed with the extinction coefficients of Cardelli et al. (1989). This technique was also applied to estimate Br γ even though the flux should in most cases be below our detection limits. The equations relating H α and H β observed line fluxes to P β and Br γ observed line fluxes under these conditions are:

$$f(Pa\beta) = 0.0141 \times AC \times f(H\alpha) \times \left(\frac{f(H\alpha)}{f(H\beta)} \right)^{1.272} \quad (1)$$

$$f(Br\gamma) = 0.0016 \times AC \times f(H\alpha) \times \left(\frac{f(H\alpha)}{f(H\beta)} \right)^{1.615} . \quad (2)$$

where $f(x)$ is the observed flux of line x . An aperture correction factor, AC, has been added to correct for the different aperture sizes used in the optical and infrared measurements. If H α /H β was not known, the median H α to H β ratio of 3.81 ($A_V = 0.53$ mag) from the other galaxies was used. In these cases the estimated values are given in parenthesis in table 3. The aperture correction between our 3" by 0.75" slit and the larger apertures in the other papers depends on the spatial extent of the line emission. We used H α + [NII] images obtained at the 60 inch telescope at Palomar (Larkin et al. 1997 in preparation), to determine the appropriate aperture correction for each object for the H α and H β measurements of Heckman et al. (1980), Keel et al. (1983) and Ho et al.(1993). For the larger circular apertures used in Heckman et al. (1980) and Keel et al. (1983), the average correction is 0.34 ± 0.04 , while the average corrections to Ho et al.'s (1993) 1" \times 4" and 2" \times 4" apertures were 0.73 ± 0.03 and 0.44 ± 0.05 respectively. The final estimated Pa β and Br γ fluxes are given in columns (4) and (5) respectively of table 3. It is important to remember that these predicted fluxes are for Pa β and Br γ as they would be measured, not corrected for extinction. The only corrections are for the difference in reddening between the optical and the infrared lines.

TABLE 3
Estimated Pa β and Br γ Fluxes and Ratios

Object	flux ($\times 10^{-15}$ erg cm $^{-2}$ s $^{-1}$)				$\frac{[FeII]}{\langle Pa\beta \rangle}$	$\frac{H_2}{\langle Br\gamma \rangle}$
	$\langle Pa\beta \text{ abs.} \rangle$	est. Pa β	$\langle Pa\beta \rangle$	$\langle Br\gamma \rangle$		
(1)	(2)	(3)	(4)	(5)	(6)	(7)
NGC 0404	2.5 \pm 0.5	1.2 \pm .6	3.1 ^b ,2.7 ^c	.55 ^b ,.49 ^c	2.7 \pm .3	5 \pm 2
NGC 2685	2 \pm .6	.5 \pm 1	(<.4) ^a	(<.06) ^a	-	-
NGC 3992	1.7 \pm .6	-.3 \pm 1	(<.3) ^a	(<.05) ^a	-	-
NGC 3998	2.2 \pm .7	1.2 \pm 1	3.6 ^a ,7.9 ^b ,4.3 ^c	.61 ^a ,1.5 ^b ,.72 ^c	.6 \pm .3	< 2
NGC 4258	2.8 \pm .9	2.4 \pm 1	(5.7) ^a	(1.0) ^a	.6 \pm .3	< 2
NGC 4589	2.5 \pm .8	0 \pm 2	(<.24) ^a	(<.04) ^a	-	-
NGC 4736	15 \pm 5	7 \pm 6	(1.9) ^c	(.35) ^c	5.3 \pm 2.5	< 20
NGC 4826	5 \pm 1	2.5 \pm 2	(6.0) ^c	(1.1) ^c	.7 \pm .4	< 1
NGC 5194	2.6 \pm .9	3.6 \pm 1	(3.1) ^b ,(2.7) ^c	(.55) ^b ,(.48) ^c	2.3 \pm .6	8 \pm 3
NGC 7217	1.8 \pm .6	.3 \pm .8	.98 ^b	.16 ^b	2.3 \pm .9	-
NGC 7479	.7 \pm .3	2 \pm .5	1.2 ^b	.26 ^b	<.5	11 \pm 4
NGC 7743	1.8 \pm .6	.6 \pm 1	3.4 ^b	.74 ^b	1.3 \pm .4	5 \pm 2

^a Flux estimated from Heckman et al. (1980).

^b Flux estimated from Ho et al. (1993).

^c Flux estimated from Keel et al. (1983).

3.2. Pa β absorption strength

Since many of the predicted Pa β emission line strengths are within the range of detectability, it is important to understand why these lines were not seen. The most likely possibility is that stellar absorption lines in the galaxies are equal to or stronger than the emission lines. In order to evaluate this possibility, we looked at the three galaxies, NGC 2685, NGC 3992, and NGC 4589, which have the weakest predicted Pa β emission line strengths (all have only upper limits on their optical H α and H β fluxes). In these three galaxies, the measured absorption is much larger than the upper limit on emission, and the emission can be assumed to have little impact on the measured values. The average equivalent width of the Pa β absorption in these three objects is $1.2 \pm 0.25 \text{ \AA}$, comparable to that seen in late G type stars. Assuming that the other galaxies in this sample have comparable or stronger absorption, column (2) of table 3 gives the lower limit on Pa β absorption for each galaxy. Adding this to the measured Pa β fluxes in table 2 gives the lower limit on the true Pa β emission line strength and these values are listed in column (3) of table 3. For all of the galaxies with Pa β seen in absorption, this fiducial absorption correction is sufficient to make the corrected values positive or zero, indicating that absorption is at least comparable to the emission line strengths, and is a plausible explanation for the nondetections.

Five of the galaxies (NGC 404, NGC 3998, NGC 4258, NGC 4826, and NGC 7743) have expected Pa β fluxes extrapolated from the measured H α fluxes which are significantly higher than these absorption corrected values. This probably indicates that the average absorption correction is too small, and these galaxies have absorption strengths closer to that found for A type stars. These galaxies may, therefore, have younger stellar populations than the three galaxies used in determining the amount of absorption. These five galaxies are among those with strong [FeII] detections. Although highly suggestive, it is important to remember that the expected Pa β fluxes are extrapolated from H α and H β measurements and unexpected factors such as unusual line ratios or patchy extinction could be affecting these values.

3.3. [FeII] and H $_2$ line ratios

As a first step in the analysis of the [FeII] and H $_2$ emission lines, we calculate the [FeII]-to-Pa β and H $_2$ -to-Br γ line flux ratios and compare them to other galaxy types in the literature. Although these line flux ratios are reddening insensitive in principle, the

$\text{Pa}\beta$ and $\text{Br}\gamma$ line fluxes are dependent on the ratio of $\text{H}\alpha$ to $\text{H}\beta$ used to infer A_V . If the extinction were very patchy towards the nucleus or had an unusual wavelength dependence, these line ratios could be biased. The ratios of $[\text{FeII}]$ to $\text{Pa}\beta$ are shown in column (6) of table 3, and the H_2 to $\text{Br}\gamma$ ratios are similarly given for each galaxy in column (7). These use the extrapolated $\text{Pa}\beta$ and $\text{Br}\gamma$ values discussed in section 3.1. In principle, these values can be treated as ratios to the optical $\text{H}\alpha$ fluxes corrected for extinction, and aperture size and then scaled to the relative $\text{Pa}\beta$ or $\text{Br}\gamma$ to $\text{H}\alpha$ intensity. This also allows for easy comparison with other emission line ratios which use $\text{H}\alpha$ or $\text{H}\beta$.

Figure 2 plots $[\text{FeII}]/\text{Pa}\beta$ versus $\text{H}_2/\text{Br}\gamma$ for the LINERs and other objects taken from the literature. It is important to remember that several of the objects such as Arp 220 and NGC 5128 (Cen A), although they are marked as LINERs and do satisfy the LINER spectral criterion, they are very different types of objects from the “Classical” LINERs included in this survey. However, it is also true that the LINER classification may apply to a diverse group of objects, and that the relation of objects like Arp 220 and NGC 5128 to the lower power LINERs may be very enlightening. Several of the LINERs have both ratios significantly higher than most other objects. For all included galaxies, regardless of galaxy type, a linear correlation is also evident over a range in ratios of more than 100. The one exception is the LINER NGC 7479 which has weaker $[\text{FeII}]$ emission than other LINERs given its large $\text{H}_2/\text{Br}\gamma$.

The points for the supernova remnants (SNR’s) in figure 2 are for small apertures on individual filaments and may not represent the global ratios in these objects. One of the SNR’s in figure 2 is the Cygnus Loop, where the excitation is thought to arise from an unusually fast shock with a magnetic precursor penetrating a low density environment (2 cm^{-3})(Graham et al. 1991). The other SNR points are from various locations in the Crab Nebula, where Graham et al. (1990) argue photoionization, not shock heating is the dominant emission source. The SNR with the largest $\text{H}_2/\text{Br}\gamma$ is IC 443, where the H_2 emission is believed to be shock excited (Graham et al. 1987).

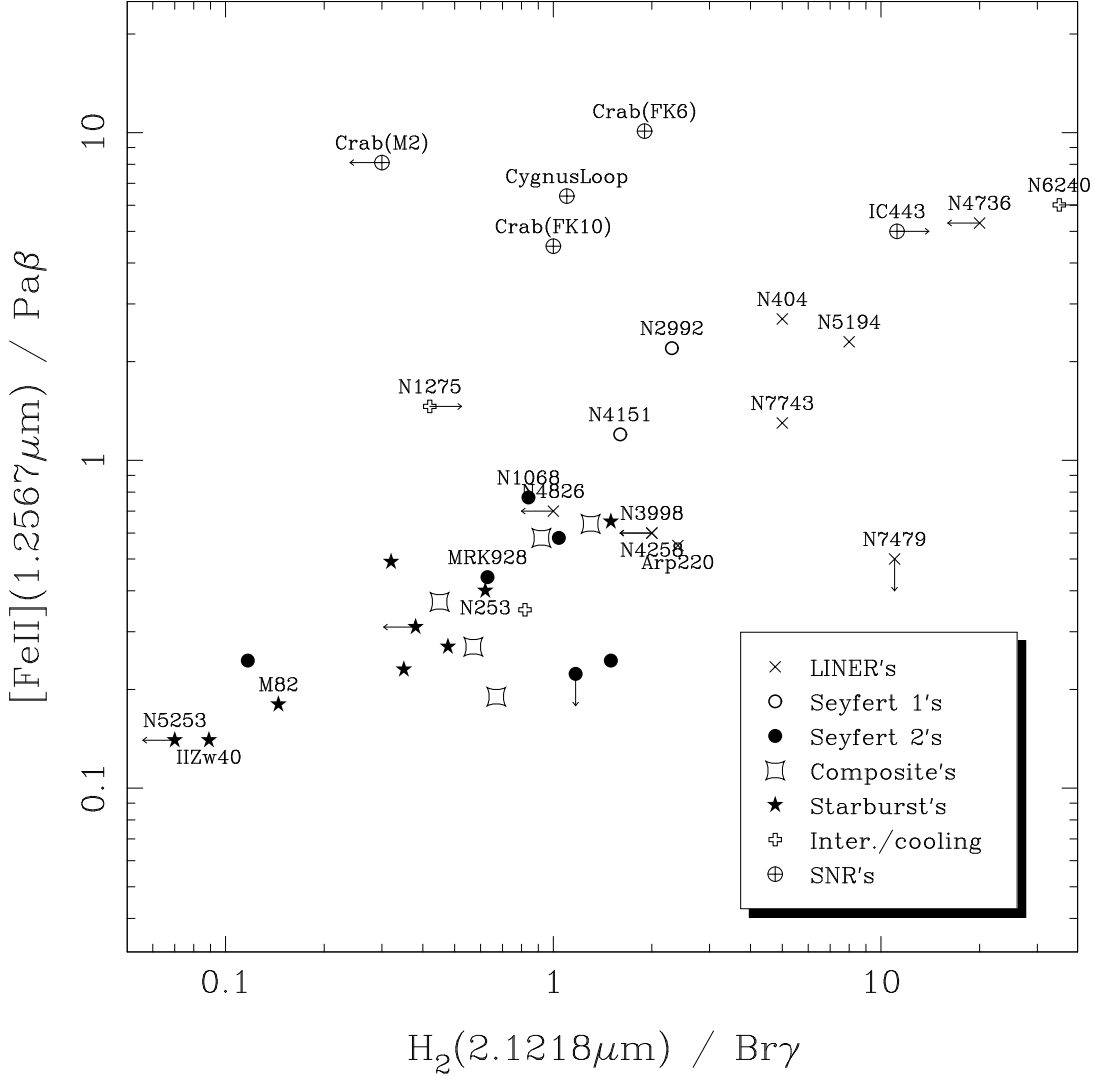


Fig. 2.— For all of the objects in this sample plus many objects from the literature, the ratio $[\text{FeII}]/\text{Pa}\beta$ is plotted against the ratio $\text{H}_2/\text{Br}\gamma$. There is a strong linear correlation between these two ratios for the galaxies included, regardless of class, even though some of the Seyfert 2's lie significantly below the correlation. Several galactic SNR's are also plotted and usually have unusually strong $[\text{FeII}]/\text{Pa}\beta$ flux ratios as compared to galaxies with similar $\text{H}_2/\text{Br}\gamma$ ratios. Also, NGC 7479, which is often classified as a Seyfert 2, is much weaker in $[\text{FeII}]$ compared to H_2 than the correlation predicts.

Figure 3 plots $H_2/Br\gamma$ versus $OI/H\alpha$ for all of the classical LINERs and for many galaxies in the literature. Mouri et al. (1989) found a linear correlation for starburst and Seyfert galaxies between the H_2 and $OI(6300\text{\AA})$ lines, and the LINERs in this sample appear to extend the linear correlation to higher values by a factor of 2 or more, although there is significant scatter. For the galaxies NGC 4258 and NGC 4826 the $OI/H\alpha$ ratio is close to that found in Seyfert galaxies and the upper limit on H_2 emission also groups the objects with Seyferts. This is not unexpected since both are considered prime candidates for dwarf Seyferts (Filippenko and Sargent 1985). Seven objects have an $H_2/Br\gamma$ ratio above 3, including 6 LINERs and the unusual object NGC 6240 which does satisfy the optical classification for a LINER. These are the only known extragalactic objects with such a large ratio of H_2 to $Br\gamma$.

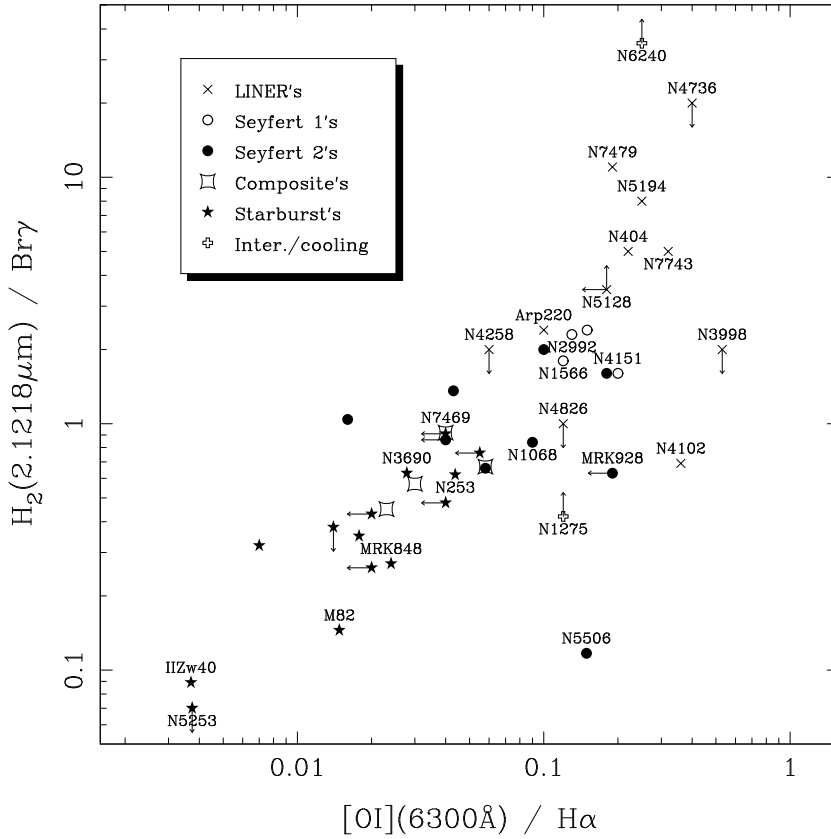


Fig. 3.— For all of the objects in this sample plus all available objects in the literature, the ratio $H_2/Br\gamma$ is plotted against the ratio $OI/H\alpha$.

Figure 4 plots $[\text{FeII}]/\text{Pa}\beta$ versus $\text{OI}/\text{H}\alpha$ for all of the classical LINERs and for many galaxies in the literature. The linear correlation seen in the previous two figures is still present, but the scatter is more apparent. Again, LINERs in general have both ratios higher than Seyferts or starbursts.

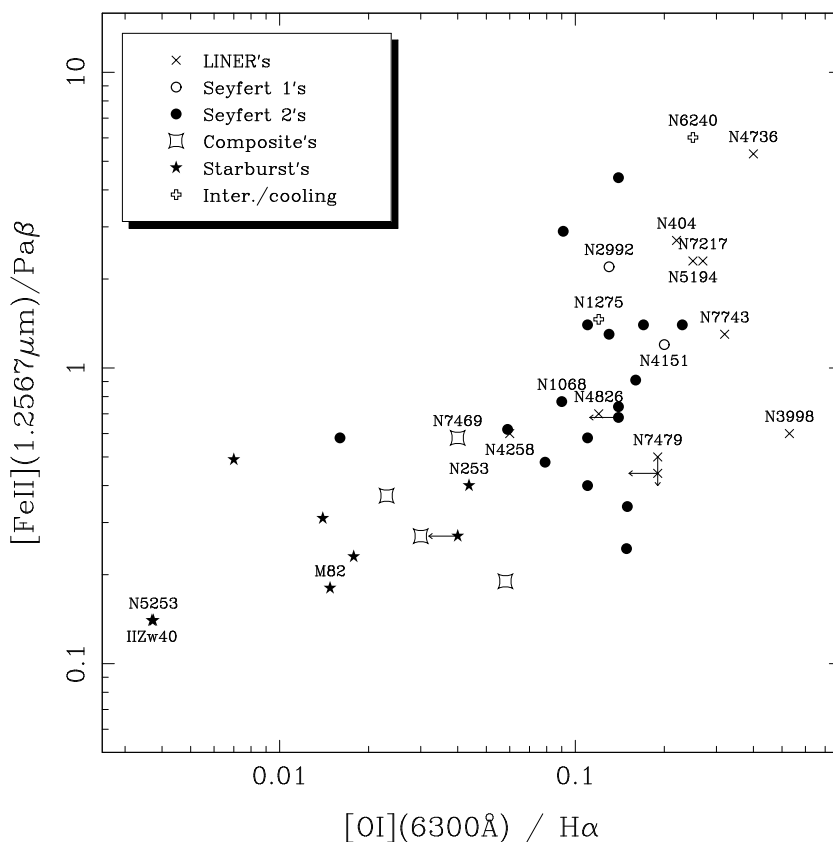


Fig. 4.— For all of the objects in this sample plus all available objects in the literature, the ratio $[\text{FeII}]/\text{Pa}\beta$ is plotted against the ratio $\text{OI}/\text{H}\alpha$. The correlation between $[\text{FeII}]$ and $[\text{OI}]$ is weaker than the correlations between H_2 and $[\text{FeII}]$ and between H_2 and $[\text{OI}]$ shown in figures 2 and 3

Figure 5 plots the optical $[\text{OIII}]/\text{H}\beta$ ratio against $\text{H}_2/\text{Br}\gamma$ for the objects in this sample and the available objects in the literature. Unlike figures 2-4, no obvious correlation is evident, however, figure 5 shows a clear separation between the LINERs and Seyfert galaxies primarily due to the difference in $\text{H}_2/\text{Br}\gamma$. As mentioned above, the six known objects with $\text{H}_2/\text{Br}\gamma$ ratios above 3 have LINER type spectra. Starburst galaxies are located in the lower left corner of these figures and are well separated from the other types. The $[\text{FeII}]/\text{Pa}\beta$ ratio is significantly poorer at separating the various galaxy classes. The $\text{H}_2/\text{Br}\gamma$ ratio is probably better at separating the classes than low ionization optical lines, because H_2 traces the colder molecular gas and is therefore less closely coupled with the high ionization lines like $[\text{OIII}]$. The three LINERs which are not grouped with the others in figure 5, all have unusual activity. NGC 4258 is a transition object with substantial recent evidence for a central black hole (see discussion of individual objects in the appendix). It is not unexpected, then that it falls within the Seyferts in this figure. NGC 4826 has an extrapolated $\text{Pa}\beta$ flux almost twice as strong as can be accounted for with the fiducial absorption applied in section 3.2. This may imply a young stellar population and recent star formation, and could explain why it is consistent with the starburst galaxies in the figure. NGC 3998, as argued below has a central source with Seyfert-like ratios, while in large apertures ($D\sim 5''$) the low ionization lines are stronger and it appears to be a true LINER. This could explain why our small aperture shows such a low $\text{H}_2/\text{Br}\gamma$ ratio, and why it lies within the range of Seyfert values.

3.4. Comparison with IRAS $\alpha(25:60)$ index

In figures 6 and 7, the IRAS 25 to 60 micron index is plotted against the $H_2/Br\gamma$ and $[OI]/H\alpha$, respectively for the LINERs in our sample and from the literature as well as many starbursts, Seyferts, composites (Seyfert + starburst), and Ultraluminous Infrared Galaxies (ULIRGS) also from the literature. The index is defined as:

$$\alpha(25 : 60) = \frac{-\log(f_{25\mu m}/f_{60\mu m})}{\log(25\mu m/60\mu m)}. \quad (3)$$

The IRAS indices measure the shape of the far infrared continuum and $\alpha(25:60)$ in particular is thought to reflect the relative importance of warm (30-50 K) dust which dominates the 60 μm band to hot (100-150 K) dust which dominates the 25 μm band. For reference, non-active galaxies have a large range of $\alpha(25:60)$, but are typically between -2 and -3. Mouri and Taniguchi (1992) found that starburst galaxies and to a lesser extent, infrared ultraluminous galaxies, showed a linear correlation between this IRAS index and $H_2/Br\gamma$. They further found that Seyfert galaxies showed no such correlation, and although some Seyferts have $\alpha(25:60)$ comparable to starbursts, most Seyferts had a shallower 25 to 60 μm slope than the starburst correlation predicts. In fact, the $\alpha(25:60)$ index has been found to be an efficient identifier of Seyfert galaxies, especially the most luminous objects where the host galaxy colors play less of a role (De Grijp, et al. 1992). The LINERs show a large spread in $\alpha(25:60)$ from NGC 3998 at -1.15 to NGC 4826 at -3.23, while showing little variation in H_2 , and $[OI]$. LINERs also show a weak trend that the objects with flatter $\alpha(25:60)$ have weaker $[FeII]$ than the steeper index LINERs. Some of the LINERs and Seyferts are close to the starburst correlations, but most have flatter indices than either the $H_2/Br\gamma$ or $[OI]/H\alpha$ would predict. ULIRGs show the opposite trend with more of them on the steeper side of the relationship, indicating an unusually large ratio of warm to hot dust.

It is interesting to point out that the LINERs with the flattest $\alpha(25:60)$ (NGC 3998, NGC 7479, NGC 7743, and NGC 4258) and are the furthest from the starburst correlation, have lower $[FeII]/Pa\beta$ than the steeper spectrum LINERs. These four objects are also the strongest candidates in the sample to have Seyfert-like nuclei (in fact NGC 7479 and NGC 4258 are often classified as Seyfert 2's). Also NGC 3998 is the strongest x-ray source among the LINER sample, and has recently been found to have an unobscured hard (1-12 keV) compact, power-law, x-ray source by ASCA (Serlemitsos 1995). For the LINERs with steep $\alpha(25:60)$ the IRAS index provides little information except that the central source does not alter the global infrared colors significantly. The majority of these sources, however, do have the highest ratios of $[FeII]/Pa\beta$.

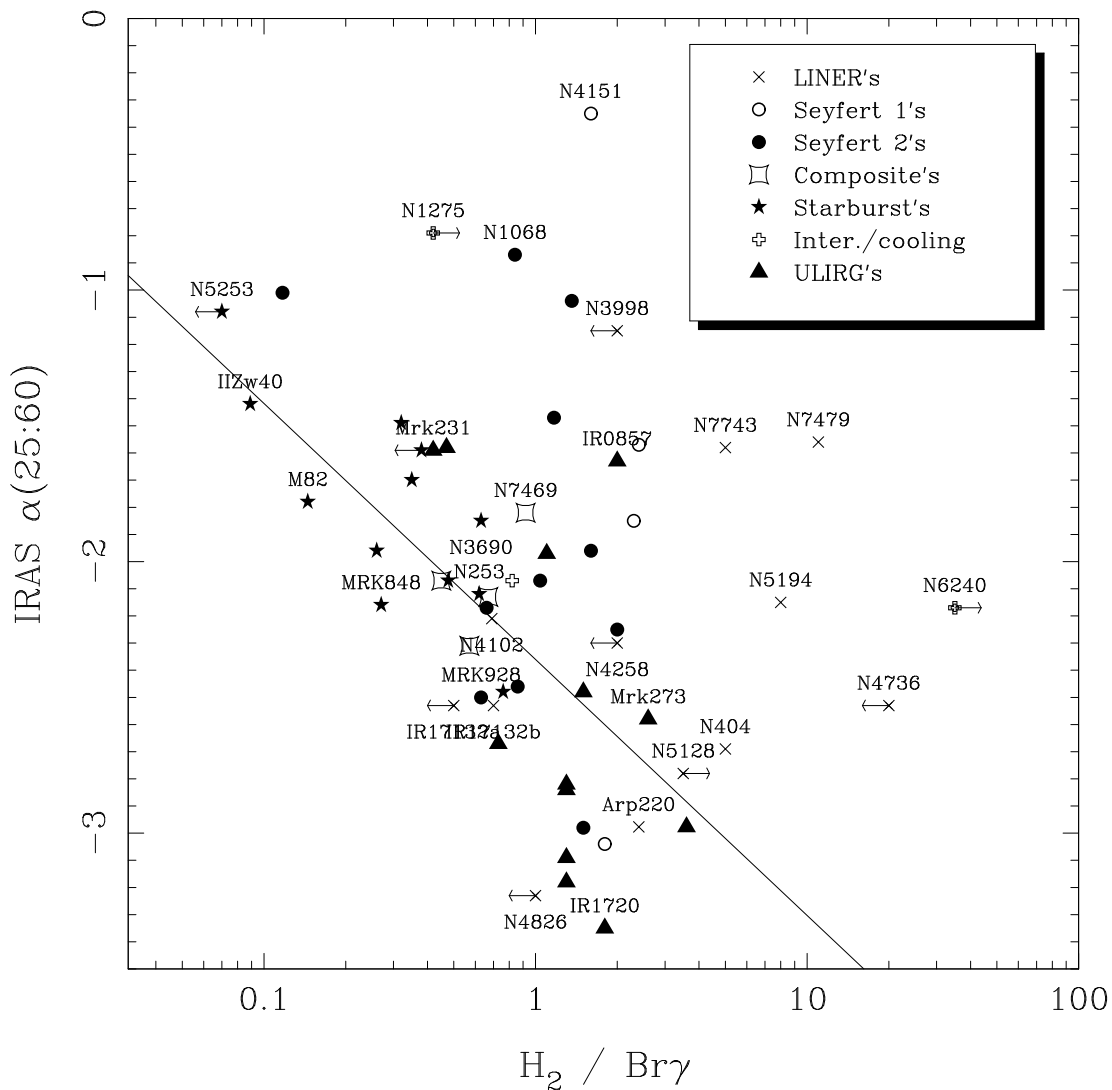


Fig. 6.— For all of the objects in this sample plus objects in the literature, the infrared spectral index from 25 to 60 μm is plotted against $H_2/Br\gamma$. A line is drawn showing the correlation between these two parameters found for starburst galaxies and ultraluminous IRAS galaxies in Mouri and Taniguchi (1992). The LINERs, like the Seyferts, do not in general follow this correlation. Again note that Arp 220 and NGC 5128 are shown as LINERs because of their spectral classification but they are much more energetic than the LINERs in this sample.

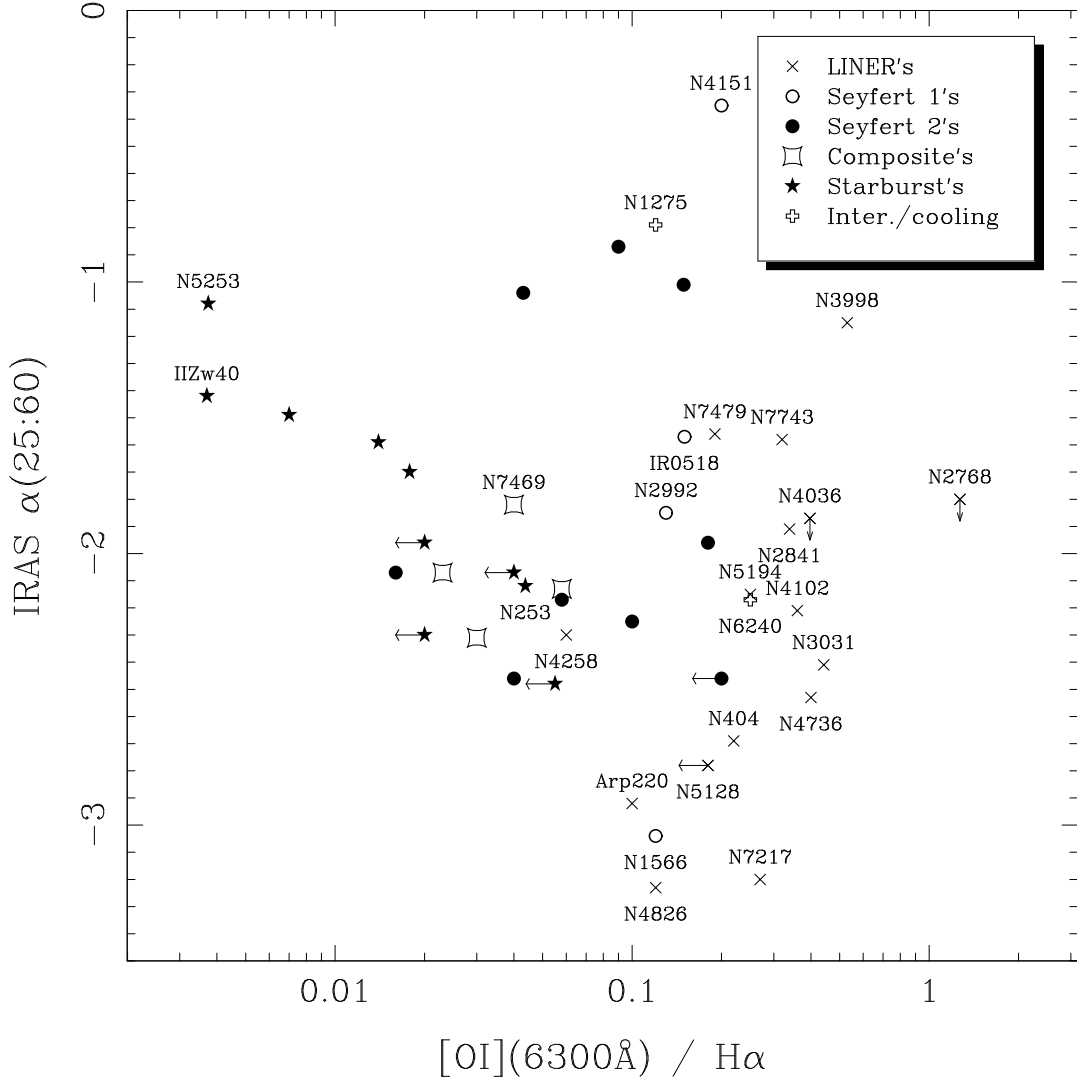


Fig. 7.— For a collection of galaxies in the literature, the infrared spectral index from 25 to 60 μm is plotted against $[\text{OI}]/\text{H}\alpha$. A linear correlation between these two parameters was found for starburst galaxies in Mouri and Taniguchi (1992). The LINERs, like the Seyferts, do not appear consistent with this correlation.

3.5. Comparison with x-ray measurements

If the LINERs with the flattest $\alpha(25:60)$, and the lowest $[\text{FeII}]/\text{Pa}\beta$ are x-ray heated by a power-law source, as in Seyfert galaxies, there should be sufficient x-rays to power the observed infrared line emission. The ratio of $[\text{FeII}]/\text{Pa}\beta$ is still relatively high in these objects, however, and some degree of grain destruction to increase the gas phase iron abundance is probably necessary. A successful x-ray heating model must therefore include a significant hard x-ray component. Unfortunately, very little is known about the hard x-ray output of LINERs. The best survey for comparison is from the Einstein satellite which operated out to 3.5 keV. For Seyfert 1's the luminosity in the range 0.5 to 3.5 keV is thought to be comparable to the hard x-ray luminosity (Van Der Werf et al. 1993).

Figure 8 plots the Einstein flux (0.2 to 3.5 keV) for the available LINERs in the sample against the total nuclear $[\text{FeII}]$ flux. To obtain the total nuclear flux, we have applied the same aperture correction discussed in section 3.1. This correction factor (roughly a factor of 3 for all objects) was determined by placing a synthetic aperture of the same width as our slit on $\text{H}\alpha+\text{NII}$ images (Larkin et al. 1997 in preparation) and comparing this to the total nuclear flux. In models of hard x-ray heating, about 1% of the 1 to 10 keV energy can come out in the $1.2567\mu\text{m}$ $[\text{FeII}]$ line. In the figure the 1% curve is plotted as a rough approximation of the minimum efficiency of x-ray to $[\text{FeII}]$ conversion. The fact that many of the Seyfert 2's are below this line probably results from dust obscuration of the soft x-ray flux. For the LINERs with Einstein detections near to or above the 1% line, there are probably sufficient x-rays to power the iron lines. As in Seyfert 2's, dust obscuration may have a significant effect on the soft x-ray fluxes of many of the LINERs making it difficult to estimate the role of x-ray heating in those objects without x-ray detections and those below the 1% line. For the five LINERs in this sample, the ratios of x-ray(.2-3.5 KeV) flux to $[\text{FeII}]$ flux are: 660 for NGC 3998; 440 for NGC 4258; 70 for NGC 4736; 70 for NGC 4826 and 175 for NGC 5194.

The first few LINERs (NGC 3998, NGC 4579, NGC 3031 (M81), NGC 4258, NGC 5194 (M51)) observed with ASCA all require a power-law x-ray source out to 12 keV, which appears to be point-like (Serlemitsos 1995). Although the current ASCA sample is not a randomly selected sample and the result is only preliminary, it does support x-ray heating in at least some LINERs.

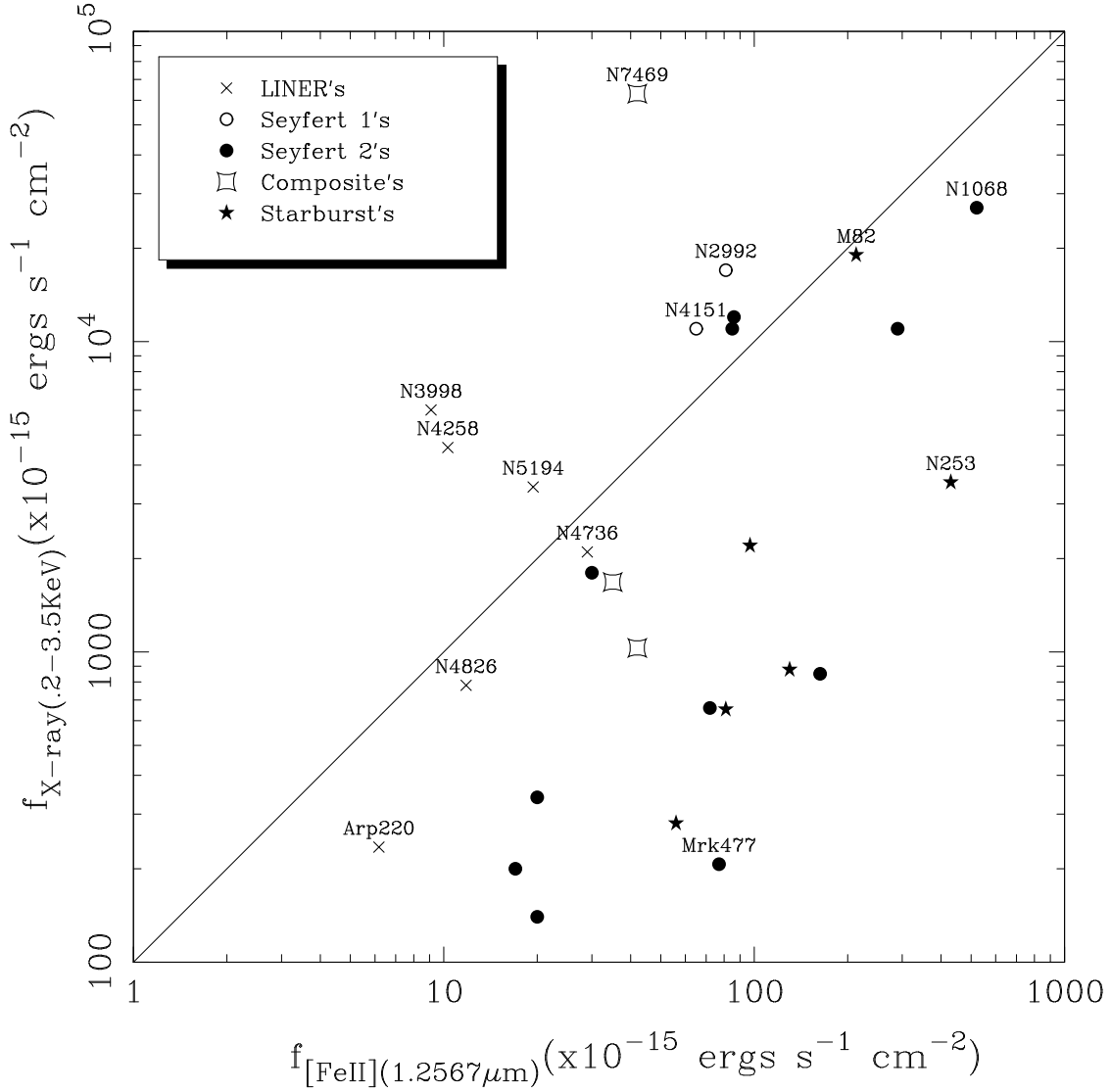


Fig. 8.— For all of the objects in this sample plus objects in the literature, the observed Einstein x-ray fluxes (.2-3.5 keV) are plotted against the total nuclear [FeII] fluxes. A line is drawn at $f_{x\text{-ray}} = 100 f_{[FeII]}$ which is approximately the fraction of [FeII] emission expected for a given $f_{x\text{-ray}}$. The total nuclear [FeII] flux is obtained by applying an aperture correction to the spectroscopic measurements as discussed in the text.

3.6. Atomic Absorption Features

In addition to the emission lines, several atomic absorption features are seen in many of the galaxies. These features were found by shifting the spectra to the rest frame and noting that several of the galaxies showed the same features. Further confidence that they are real features in the galaxies' spectra and are not a reduction artifact comes from a comparison with optical spectra in Filippenko and Sargent (1985) which show that the galaxies with the strongest infrared absorption lines also have the strongest optical absorption lines. In figure 1, these suspected absorption lines are marked by vertical marks at the top of each panel with the most likely identification given. The line identifications were found by comparing the spectra with a very high resolution ($R \sim 100,000$) spectrum of the solar photosphere (Hall 1973). Among the strongest lines present in the galaxies spectra are a Na doublet ($\lambda\lambda 2.2062, 2.2090 \mu\text{m}$) and a Mg doublet ($\lambda\lambda 1.2423, 1.2433 \mu\text{m}$). The Na doublet is seen in all seven galaxies where the spectra extend to this wavelength. One feature at $\lambda_{rest} = 1.2893 \pm 0.0003 \mu\text{m}$ is still not identified, although it is detected in 5 or 6 of the galaxies. It is possible that this line is from a molecular species present in cool giants but not in the Sun.

4. Discussion

The most striking feature of the infrared spectra is the strength of the [FeII] and H_2 features in relation to hydrogen recombination lines, and the correlation of H_2 and [FeII] with the optical [OI] line. Ho et al. (1993) found that there was a clear separation between LINERs and transitional objects at $[\text{OI}]/\text{H}\alpha \sim \frac{1}{6}$. We find a similar separation between the majority of LINERs in this sample and Seyferts at $[\text{FeII}]/\text{Pa}\beta$ of ~ 1 , and $\text{H}_2/\text{Br}\gamma$ ratio of ~ 3 . This transition is clearer than the difference in [OI]/ $\text{H}\alpha$ ratios for LINERs and Seyferts. The one galaxy which does not satisfy this is NGC 3998, which as argued above, satisfies the LINER criterion only for larger apertures than employed here, and which is Seyfert-like in small apertures. In this object at least, the LINER classification may be based solely upon circumnuclear emission lines which may be photoionized or shock heated by a central AGN.

The $\text{H}_2/\text{Br}\gamma$ ratio also divides the Seyfert's from the starburst galaxies in the literature at ~ 0.6 , although several exceptions are evident. It is therefore, interesting to consider that $\text{H}_2/\text{Br}\gamma$ can alone be used to classify galaxies as either starbursts, Seyferts (and transitional LINERs), and LINERs. Figure 5 shows that by including the $[\text{OIII}]/\text{H}\beta$ ratio, the divisions

between these classes become even clearer. It must, however, be remembered that these trends apply only when the true Pa β and Br γ emission line fluxes free of stellar absorption are available or can be estimated with reasonable precision. This is particularly important for LINERs where the stellar features often dominate the nuclear activity even for small apertures.

4.1. Possible Sub-Classes

An interesting result of this work is that the LINERs with infrared line detections break up into basically two groups based on the ratio of [FeII] to Pa β . In the following, LINERs with [FeII]/Pa β above 2 will be referred to as “strong” [FeII] LINERs, while the ones below 2 will be called “weak” [FeII] LINERs. The [FeII]/Pa β line ratio uses the extrapolated Pa β line fluxes discussed in section 3.1. If the extinction towards the nucleus were very patchy it could affect these extrapolated values and therefore the classification scheme. Since most of the galaxies are either nearly face on spirals or ellipticals with little dust, we don’t believe this is a large affect. The line ratios can equally be thought of as the ratio of [FeII] to H α corrected for the measured extinction between H α and H β .

The “weak” [FeII] LINERs include NGC 4826, NGC 3998, NGC 4258, NGC 7479 and NGC 7743. All three of the LINERs with relatively flat far infrared spectra ($\alpha(25:60) > -2$) are “weak” [FeII] LINERs. Although the interpretation of the $\alpha(25:60)$ index is complicated, a flatter spectrum probably indicates a strong nuclear source that is able to alter the global dust temperatures and affect the IRAS colors. The only two LINERs with detected broad H α lines (NGC 3998 and NGC 4258) are “weak” [FeII] LINERs. These two LINERs are also the strongest x-ray sources in the sample and have the highest ratios of x-ray flux to [FeII] flux. The other three “weak” [FeII] LINERs also show evidence for Seyfert-like activity. Technically, NGC 7479, should actually be classified as a Seyfert 2 based on its optical line ratios. NGC 7743 also has unusual line ratios with the highest [OIII]/H β ratio in the sample indicating a relatively high state of ionization. The last “weak” [FeII] LINER, NGC 4826 is technically a “weak” [OI] LINER since [OI]/H α is less than $\frac{1}{6}$, and it has the lowest H $_2$ /Br γ ratio in the sample.

The “strong” [FeII] LINERs are NGC 404, NGC 4736, NGC 5194 and NGC 7217. None of the “strong” [FeII] LINERs has a detected broad H α line, and none are known as strong x-ray sources. Among the “strong” [FeII] LINERs, NGC 404 and NGC 4736 are particularly noteworthy for having unusually strong Balmer absorption lines indicative of recent star formation. NGC 4736 and NGC 7217 also have inner rings or arcs of H α

emission probably resulting from circumnuclear star formation. NGC 5194 was classified by Heckman (1980) as a transition object (its oxygen line ratios are on the border between Seyfert and LINER classifications). It does, however, have a high ratio of $[\text{FeII}]/\text{Pa}\beta$ (2.3) and a very strong H_2 line ($\text{H}_2/\text{Br}\gamma = 8$). Because NGC 5194 is closer to a Seyfert in optical line ratios, and because it has a good x-ray detection, however, it is not as consistent with star formation as the other “strong” $[\text{FeII}]$ LINERs. All of the “strong” $[\text{FeII}]$ LINERs have steep ($\alpha(25:60) < -2$) IRAS indices.

An appealing model is that the two groupings reflect different excitation mechanisms (See the following subsection). The “weak” $[\text{FeII}]$ LINERs may be low luminosity Seyferts, while the “strong” $[\text{FeII}]$ LINERs may be powered by compact starbursts. Compact supernova remnants (pressure confined) are likely to enhance the $[\text{FeII}]$ line in the latter group. The $[\text{FeII}]$ luminosities of several of the galaxies, in particular the “strong” $[\text{FeII}]$ LINERs NGC 404 and NGC 4736, are only a few times those expected for individual supernova remnants, making supernovae, an attractive excitation source. Although this model of “strong” and “weak” $[\text{FeII}]$ LINERs is attractive it is by no means definitive, since none of the objects in either sample is unambiguously a Seyfert-like or starburst-like nucleus. The next subsection also shows that x-ray heating from a central Seyfert-like source can reproduce the large $[\text{FeII}]/\text{Pa}\beta$ ratios of “strong” $[\text{FeII}]$ LINERs under special conditions. It is, however, suggestive that the LINERs with the strongest indications of recent star formation have the greatest $[\text{FeII}]/\text{Pa}\beta$ ratios. It is possible that the “strong” $[\text{FeII}]$ LINERs have a Seyfert-like core, but also have a surrounding star formation region where supernova remnants enhance the $[\text{FeII}]$ emission.

4.2. Excitation of the $[\text{FeII}]$ and H_2 emission

The main goal of this study was to characterize the infrared spectra of LINER galaxies with the further goal of determining the source of the strong, low ionization emission lines in LINER spectra. The observation that both the molecular line H_2 1-0 S(0) and the $[\text{FeII}]$ line are strong, places stringent requirements on the excitation mechanism since (1) H_2 is relatively easy to destroy, and (2) 98% of the iron is tied up in dust grains in the local ISM. In order for a common mechanism to power both lines, as well as the optical $[\text{OI}]$ line, it must not destroy all of the H_2 molecules and yet must free up iron through dust grain destruction. The strength of the $[\text{FeII}]$ line is much harder to explain through increased metallicity, since the oxygen, nitrogen and sulfur lines in the optical are not consistent with extremely high metallicities.

A general equation for the strength of [FeII] versus Pa β is derived from Blietz et al. (1994) and is given by:

$$\frac{[FeII](1.2567\mu m)}{Pa\beta} = coef \times \delta \times \left(\frac{f_{II}}{\xi}\right) \quad (4)$$

where

$$coef = \frac{22 \times T_4^{0.07} \times \exp\left(\frac{-1.57}{T_4}\right)}{\left[1 + 4.2 \times \left(\frac{T_4^{0.69}}{n_4}\right)\right]}$$

where T_4 is the temperature in units of 10^4 K, n_4 is the electron density in units of 10^4 cm^{-3} , δ is the fraction of iron in the gas phase, f_{II} is the fraction of gaseous iron that is singly ionized, and ξ is the ionization fraction of hydrogen. The coef term is provided for convenience to separate the temperature and density dependence from the dependences on iron abundance and ionization states. This equation is of course only valid if both lines arise within the same parcel of gas. If multiple excitation mechanisms exist, then the equation can still be used to try and constrain the dominant mechanism.

Since δ is ~ 0.02 in the local ISM, even for the most extreme possible temperature and density for these objects, $coef \times \delta$ is only 0.5. So unless the gas phase abundance of iron is much greater than locally, and/or the ionized fraction of iron to hydrogen is much greater than 1, then [FeII]/Pa β cannot reach the level of the “strong” [FeII] LINERs.

Several types of environments can immediately be ruled out based on equation 4. Standard HII regions have a fraction of Fe $^+$ to hydrogen of less than ~ 0.2 (Oliva et al. 1989). In order to reach [FeII]/Pa β of even the values of ~ 0.6 seen in the “weak” [FeII] LINERs requires the gas phase abundance of iron (δ) to be 0.12 (a six fold increase in gas phase iron) for even the most extreme conditions ($T = 10^5$ K and $n = 10^5$ cm^{-3}). For more reasonable conditions ($T = 10^4$ K and $n = 10^4$ cm^{-3}), δ must be greater than 1, which is unphysical. Even δ of 0.12 is difficult to explain in an HII region, since there are no strong mechanisms to process dust grains. Since Galactic HII regions are observed to have very weak [FeII] emission, it is expected that extragalactic HII regions should have [FeII]/Pa β ratios much less than unity.

The photodissociation region around strong UV sources were also examined by Blietz et al. (1994) since these regions can produce strong H $_2$ and other low ionization lines. The temperatures in the photodissociation regions are always below 2000 K, however, which greatly reduces the [FeII] flux ($coef < 1$). Also these regions tend to be very thin, so the ratios of low ionization lines to hydrogen recombination lines (which are generated interior to the ionization fronts) is in general very low.

X-ray heating from a nonthermal power-law source can produce an extended ionization front if very hard x-rays are present (Halpern and Grindlay 1980). In such extended regions, the fraction of ionized iron to hydrogen can reach 100, although the temperature may be only ~ 3000 K (Blietz et al. 1994). For this temperature, the coef parameter is about 0.11 for any density over $\sim 10^4$ cm^{-3} . For a ratio of $[\text{FeII}]/\text{Pa}\beta$ as high as 2, δ must be at least 18%. Although high, this is not unfeasible since hard x-rays can destroy dust grains. For the “weak” $[\text{FeII}]$ LINERs, the ratio of $[\text{FeII}]/\text{Pa}\beta$ of ~ 0.6 , δ need only be 0.055, which is very reasonable. X-rays are therefore an attractive emission source for the “weak” $[\text{FeII}]$ LINERs and may play a part in powering the infrared emission lines in the “strong” $[\text{FeII}]$ LINERs as well.

Another possible excitation mechanism is a J-type shock (jump discontinuity shocks without magnetic precursors). Shocks can produce large fractions of ionized iron to hydrogen and provide a natural mechanism for dust grain processing. Seab and Shull (1983) find that fast shocks (40 to 120 km s^{-1}) can increase the gas phase iron abundance (δ) up to 60%. For an expected ionization fraction of iron to hydrogen of around 2, J-shocks then require coef to be greater than 1.7 for $[\text{FeII}]/\text{Pa}\beta$ around 2, and 0.5 for $[\text{FeII}]/\text{Pa}\beta$ of 0.6. These values are possible for virtually any temperature above 10^4 and density above 10^4 . This fact makes shocks a very attractive mechanism for the “strong” $[\text{FeII}]$ LINERs, and they may also produce the $[\text{FeII}]$ emission in the “weak” $[\text{FeII}]$ LINERs. If present in “weak” $[\text{FeII}]$ LINERs, the effect of shocks is probably diluted by other mechanisms. Although fast shocks will destroy H_2 , there may exist a range of gas densities making a variety of shock speeds possible. The strong H_2 lines may then result from the same shock mechanism that produces the $[\text{FeII}]$ emission, but in different parts of the gas.

Both hard x-ray heating, and fast shocks are plausible mechanisms for all of the LINERs, although the “weak” $[\text{FeII}]$ LINERs are easier to explain by x-ray heating while “strong” $[\text{FeII}]$ LINERs are more consistent with shock excitation. Both mechanisms are also able to generate the H_2 emission, but shocks are more efficient at $[\text{FeII}]$ production, and are better able to explain the “strong” $[\text{FeII}]$ LINERs. If shocks are present, either compact supernova remnants (pressure confined), or other mechanisms such as cloud-cloud collisions, or outflowing winds are plausible shock sources. Supernova remnants are the likely source for the “strong” $[\text{FeII}]$ LINERs since many of these show other evidence for recent star formation.

4.3. Possible Biases

In any survey of a small sample of objects with faint emission features, biases in selection, photometry and aperture correction, sensitivity and a large number of other sources may play a significant role. In this subsection we discuss some of the most obvious sources of bias, and try to estimate their effects.

One of the largest biases affecting this survey is the size of the sample and the fact that the line detections are preferentially in the most active LINERs; the others are too faint. A significant population of LINERs have featureless infrared spectra and cannot be addressed by the infrared diagnostics. For most quantities discussed, there is a relatively smooth transition from LINER-like spectral properties to Seyfert-like. An important consideration is that the least active LINERs, which have no line information, are less like Seyfert's in their emission mechanism than those discussed in detail, and many of the correlations may not hold for these LINERs. We have tried, in a limited fashion, to address this problem by also using the optical [OI](6300Å) line, which is well correlated with the infrared lines for all LINERs, in examining the excitation mechanisms. Since this line must be detected for a galaxy to be classified as a LINER according to the original definition, it does not suffer from the same selection bias. However, it is possible that the [OI] emission does not arise from the same regions as the infrared lines.

Another bias is the lack of hydrogen recombination line detections. Since we are applying optical extinction estimates to extrapolate the intrinsic strengths of the near infrared features, we may be subject to large uncertainties if the extinctions to the optical and IR emitting regions are significantly different. If the extinction to the infrared lines were higher than predicted from $H\alpha$ and $H\beta$, then the estimated infrared recombination lines would be too low, and the corresponding ratios with [FeII] and H_2 too high. Since the extrapolated [FeII]/ $Pa\beta$ and $H_2/Br\gamma$ line ratios correlate with the [OI] line, it is not likely that the recombination strengths have been severely underestimated. Also, since the extrapolated values of $Pa\beta$ and $Br\gamma$ from optical lines are typically higher than can be accounted for by correcting the observed spectra for stellar absorption, it is more likely that $Pa\beta$ and $Br\gamma$ have been overestimated which would imply that the line ratios are even higher than calculated. A logical next step will be to obtain high signal to noise infrared spectra of several template galaxies for subtraction in order to identify extremely weak emission lines lost in stellar absorption features.

It is possible that the difference in size between our aperture and those used in the optical plays a role in increasing the observed [FeII] and H_2 ratios. Knop (personal communication 1997) has used a similar small aperture to measure the infrared line ratios

in some nearby Seyfert galaxies and has found that many of them have slightly higher [FeII] and H₂ flux ratios than Seyferts in the literature, but the effect is much too weak to account for the differences seen between the LINERs and the Seyferts. There is one object (NGC 2110) in the Knop sample, however, which is a Seyfert with a very large [FeII] to Paβ flux ratio of 8, and an H₂ to Brγ flux ratio of 3. This object is extremely interesting but does not reflect the ratios typically observed for Seyfert galaxies in small apertures. In fact, several of the LINERs that have multi-aperture optical spectra, show stronger low ionization lines in the larger aperture, which implies just the opposite effect.

In general, we believe that the biases and observational limitations present in the data do not alter the interpretation of the physical processes at work in LINER nuclei.

5. Summary and Conclusions

This paper has described an infrared spectroscopic survey of 12 “classical” LINER galaxies. The spectra have concentrated on the [FeII](1.2567μm), Paβ, H₂(2.1218μm) and Brγ infrared lines. The major results are:

1. [FeII] and H₂ are the strongest infrared lines in classical LINERs. Using extrapolated H⁺ line strengths from the optical, approximately half of the classical LINERs have ratios of [FeII]/Paβ and/or H₂/Brγ a factor of two or more higher than typical Seyfert galaxies and a factor of five or more higher than typical starburst galaxies.
2. A natural subdivision between the LINERs occurs at [FeII]/Paβ = 2. The four “strong” [FeII] LINERs exhibit evidence for recent or ongoing star formation. As a group, the [FeII] emission in these LINERs is consistent with shock excitation from compact supernova remnants. The five “weak” [FeII] LINERs have more in common with Seyfert galaxies, including the only two objects in the sample with broad Hα (NGC 3998 and NGC 4258). The lower [FeII]/Paβ and H₂/Brγ ratios of “weak” [FeII] LINERs are consistent with hard x-ray heating from a power-law source. Neither excitation mechanism is ruled out for either type of object, however, and it is possible that it is just the relative strengths of the two mechanisms that are different in the two groups.
3. In most of the LINERs, the estimated amount of Paβ absorption from the stellar population can account for the lack of Paβ detected in emission. Several of the LINERs have unusually strong Paβ absorption (>2Å EQW) indicative of younger

stellar populations. The five galaxies with the strongest absorption all have strong [FeII] lines and supernova remnants from recent star formation are a plausible explanation for their enhanced [FeII] strengths.

4. A strong linear correlation is observed between $H_2/Br\gamma$, $[FeII]/Pa\beta$ and $[OI]/H\alpha$ for a range of 100 in all ratios and for all of the observed galaxy types. However, the “strong” [FeII] LINERs are stronger in [FeII] than the correlation with [OI] predicts. Both the $H_2/Br\gamma$ and to a lesser degree the $[FeII]/Pa\beta$ ratio, appear to separate the three galaxy classes: LINERs, Seyferts and starbursts. Only six objects have been observed to have $H_2/Br\gamma$ higher than 3, and all are LINERs. In conjunction with the $[OIII]/H\beta$ ratio, the class distinctions are even clearer.
5. The shallow far infrared spectral slopes of some of the “weak” [FeII] LINERs in comparison to the strengths of H_2 and [OI], appear inconsistent with the correlations observed for starburst and ULIRG galaxies. This argues very strongly that a nonthermal heat source is providing much of the dust heating and line excitation for these objects.
6. LINERs with x-ray detections appear to have sufficient x-ray luminosity to power the observed infrared lines. Starbursts often have [FeII] and H_2 lines many times stronger than the x-rays luminosity should be able to produce. Again the strong x-ray LINERs do not appear consistent with star formation, but instead behave like mini-Seyferts.

The authors would like to thank Thomas Murphy, Gerry Neugebauer, David Shupe, and Alycia Wienberger for many useful discussions on these results. We also want to thank Roger Blandford and Nick Scoville for many helpful comments. Special thanks goes to the Palomar night assistants, Skip Staples, Juan Carasco and the entire Palomar staff. This research has made use of the NASA/IPAC Extragalactic Database (NED) which is operated by the Jet Propulsion Laboratory, Caltech, under contract with NASA.

Individual Objects

NGC 404 : A classical LINER fully satisfying the Heckman (1980) criteria. The infrared spectra show very prominent [FeII] emission and a strong detection of H₂. NGC 404 has the largest [FeII] line to continuum ratio for any of the LINERs in this sample. It is plausible that the estimated Pa β flux is too high and that the calculated [FeII]/Pa β flux is significantly higher than the value of 2.7 in table 3. Even with this large estimated Pa β flux, NGC 404 has one of the highest ratios of [FeII] to Pa β of any extragalactic object. The apparent feature at the location of Br γ is due to residual ripple in the G star spectrum used to remove telluric absorption which is most apparent in NGC 404 because it is at essentially zero redshift. Since the expected Br γ is below the detection limit, and there is an obvious explanation for the feature, we do not regard this as a real detection of Br γ in NGC 404. All of the line emission is spatially unresolved with a seeing of 1". At a distance between 1.8 and 2.4 Mpc, this corresponds to only 10pc. At this distance, the aperture corrected [FeII] luminosity is 1.1×10^{37} ergs s⁻¹ which is only a few times the expected luminosity for a single supernova remnant (Moorwood and Oliva 1988). It is an interesting possibility that the emission within NGC 404 could be generated in a single SNR in a high density medium. The Pa β absorption correction, estimated in subsection 3.2 is about a factor of two too low to explain why Pa β is undetected. The most obvious explanation is that NGC 404 contains a significant population of young stars which increase the amount of Balmer absorption. This is supported by Keel (1983), who considered NGC 404 a peculiar member of the LINER class due to the presence of a blue continuum and strong Balmer absorption lines. NGC 404 shows none of the infrared atomic absorption features seen in some of the other galaxies in this sample. The optical spectrum, (Filippenko and Sargent, 1985) also shows a relatively smooth continuum spectrum. Although the emission lines are very narrow, a strong central UV point source and several surrounding fainter UV sources have been detected with HST (Maoz, 1993). Although the central UV source was taken as evidence for an AGN by Maoz, a central star cluster is also a possibility.

NGC 2685 : Classified as a LINER based upon only the [OII]/[OIII] ratio, this object has very weak optical lines. No emission lines are detected in the infrared spectrum. There appears to be a strong Pa β absorption feature, although the continuum around it has residual features from the night sky and the G star division. It does show most of the atomic absorption features, especially the Mg ($\lambda\lambda 1.2423, 1.2433\mu\text{m}$) and Na ($\lambda\lambda 2.2062, 2.2090\mu\text{m}$) lines. Optically it has strong Balmer absorption, weak NII and strong atomic absorption lines (Filippenko and Sargent 1985).

NGC 3992 (M 109) : Like NGC 2685, it was classified as a LINER solely on the basis of the [OII]/[OIII] ratio. No emission lines are detected in the infrared spectrum. There is an

obvious strong Pa β absorption line. NGC 3992 also shows the strongest atomic absorption features of the classical LINERs in this sample. The spectrum in Filippenko and Sargent (1985) also shows prominent atomic absorption features and weak emission lines.

NGC 3998 : A true LINER which shows increasing ratios of [OI] and [OII] to [OIII] with increasing aperture size. The only detected infrared emission line is [FeII] which is detected at the 4 to 5 sigma level. Using the estimated Pa β flux, the ratio of [FeII] to Pa β is 0.6, which is one of the lowest in the sample. H₂ is undetected, setting a low limit for the H₂/Br γ ratio. Both of these ratios are significantly lower in comparison to the OI/H α ratio than the other LINERs in the sample. The limit of the ratio of H₂ to [FeII], however, does lie along the main correlation for LINERs and other galaxies. In Larkin et al. (1997, in preparation), it is argued that the NII emission is significantly extended in comparison to the H α . It is probable that the OI, and also probably the [FeII] and H₂, are also more extended than the H recombination lines, and that the optical ratio calculated in the larger aperture is enhanced in comparison to the infrared ratios in a much smaller aperture. If true, then the infrared ratios in a larger aperture would probably be greater and NGC 3998 would lie closer to the main correlations shown in figures 2 and 3. In principle, this says that the low ionization lines are more extended than H α , and that the unresolved core has more Seyfert-like line ratios. The Na and Mg absorption features may be present at a very low level. Optical spectra show prominent broad H α wings and even a broadened [OI] line (700 km sec⁻¹). Optical absorption features, if present, are weak and broadened (Filippenko and Sargent 1985). Like NGC 404, NGC 3998 has had a strong UV point source detected by HST (Fabbiano et al. 1994). Coupled with the broad H α , this makes NGC 3998 a prime candidate for a low luminosity Seyfert galaxy.

NGC 4258 (M 106) : One of Heckman's original two transitional objects. Its optical line ratios are actually typical of Seyferts. Its infrared spectra are similar to those of NGC 3998; only a fairly weak detection of [FeII] in emission. It also has a ratio of [FeII] to Pa β ratio of 0.6, which is low for this sample, but similar to NGC 3998. Optically, is also very similar to NGC 3998, with faint broad wings of H α and slightly broadened OI. The Na absorption feature is detected weakly. Unlike NGC 3998, NGC 4258 shows several strong optical absorption features (Filippenko and Sargent 1985). A wealth of high resolution observations have focused on NGC 4258, showing it to have a rotating ring of water masers (e.g. Nakai et al. 1993), optical jets (e.g. Ford et al. 1986) and a steeply rising velocity curve (Miyoshi et al. 1995), all of which make NGC 4258 one of the best candidates for harboring a central black hole. Its [FeII] and H₂ ratios are comparable to Seyferts.

NGC 4589 : Classified as a LINER based on only the [OII] to [OIII] ratio. This is the most featureless of the LINERs in the infrared, showing no emission or absorption

lines, except possibly weak $\text{Pa}\beta$ absorption. Mollenhoff and Bender (1989) showed that NGC 4589 had a peculiar velocity field with evidence for large streaming motions, and a warped dust lane. They argued that NGC 4589 was the result of a recent merger.

NGC 4736 : A true LINER satisfying both of Heckman’s (1980) criteria. NGC 4736 is one of the strongest continuum sources in the sample making the weak lines difficult to detect. The $[\text{FeII}]$ to $\text{Pa}\beta$ ratio is the highest of any object in this sample, and the second largest of any extragalactic object measured (only NGC 6240 has a higher ratio). This ratio is, however, uncertain by 50% due to the strong continuum surrounding the $[\text{FeII}]$ line and the strong $\text{Pa}\beta$ absorption. The ratio is supported by the strong optical ratio of $[\text{OI}]/\text{H}\alpha$ which, as discussed above, is correlated with $[\text{FeII}]/\text{Pa}\beta$. The $\text{H}_2/\text{Br}\gamma$ is only a very poor upper limit, but based on the other two line ratios, is probably also very high (~ 10). Like NGC 404, NGC 4736 is very close (4.3 Mpc) making the $[\text{FeII}]$ luminosity only a few times higher than an individual SNR. The estimated $\text{Pa}\beta$ absorption in table 3 is not sufficient to reconcile optical line strengths and the observed $\text{Pa}\beta$ flux. This may indicate the presence of a younger stellar population. Atomic absorption features are strong in the infrared spectra, and in the optical spectra of Filippenko and Sargent (1985). NGC 4736 was found to have two compact UV sources separated by $2.5''$ in its nucleus by HST (Maoz et al. 1993). It also had UV arcs at $2''$, $4''$ and $6''$ suggestive of bow shocks. At much larger scales, NGC 4736, has a strong ring of $\text{H}\alpha$ emission (Larkin et al. 1997, in preparation). All of these features suggest that NGC 4736 has experienced recent star formation.

NGC 4826 (M 64): Probably a true LINER since $[\text{OI}]/[\text{OIII}] = 0.65$ (Keel 1983), but $[\text{OII}]$ is not measured. The infrared spectra look very similar to NGC 4736, with the relatively weak $[\text{FeII}]$ detection, and fairly strong atomic absorption features. A strong $\text{Pa}\beta$ absorption line is also apparent. Optical spectra from Filippenko and Sargent (1985) show strong emission lines, many atomic absorption features, but no broad $\text{H}\alpha$. Along with NGC 4258 and NGC 3998, it has the lowest ratios of $[\text{FeII}]$ and H_2 to hydrogen lines of this sample, and their ratios are actually located within the range typical of Seyferts.

NGC 5194 (M 51) : One of Heckman’s (1980) original transition objects with oxygen line ratios comparable to Seyferts. Among the most famous LINER galaxies, M 51 is one of only two in this sample to show $\text{Pa}\beta$ in emission (although it is very weak). M 51 also shows strong $[\text{FeII}]$ and H_2 emission and has estimated ratios among the highest in this data set, significantly above any Seyfert or starburst galaxy. A bubble of $\text{H}\alpha$ emission is seen just off of the nucleus (Larkin et al. 1997, in preparation). Known as the whirlpool galaxy, it has an obvious interaction with NGC 5195 which may contribute to any nuclear activity. No broad lines are detected by Filippenko and Sargent (1985). The only obvious atomic absorption feature in M51 is the Na doublet, although Mg may also be present.

NGC 7217 : A true LINER satisfying both of Heckman’s criteria. Only a J-band spectra is available for NGC 7217. It shows strong [FeII] in emission, and Pa β in absorption, along with faint atomic absorption features. It ranks among the top four LINERs in [FeII]/Pa β ratio. In H α , an inner ring of radius 10” is visible suggesting some form of recent tidal interaction or star formation (Larkin et al. 1997, in preparation). Filippenko and Sargent (1985) found no broad H α component and only weak atomic absorption.

NGC 7479 : NGC 7479 does not meet the full LINER classification of Heckman (1980) in the small aperture of Ho et al. (1993) since [OI]/[OIII] is below 1/3rd, but it has [OI]/[OIII] of $\sim \frac{2}{3}$ in Keel’s larger 6” aperture. It is also often classified as a Seyfert 2 in the literature. NGC 7479 is the only galaxy in this sample to be detected in H₂ but not in [FeII]. It also has a strong Pa β emission line detected. The small features near the wavelength of Br γ are probably residual fringes from the calibration G star spectrum and are not believed to be line detections. Filippenko and Sargent (1985) found no broad H α , although many of the lines showed a complex velocity field which suggests a fuel supply of molecular gas. Since the [OI] may be more extended than the [OIII] emission, the central source may have Seyfert-like line ratios.

NGC 7743 : It has a [OI]/[OIII] ratio of 0.14 which is below the cutoff of $\frac{1}{3}$ of Heckman (1980) but it has strong [OII] emission. The infrared spectra show strong [FeII] and H₂ emission lines, and perhaps broadened Pa β and Mg absorption lines. Its [FeII] and H₂ ratios are significantly stronger than Seyfert and starburst galaxies. Filippenko and Sargent (1985) found no broad H α component and a fairly smooth continuum with little atomic absorption.

REFERENCES

- Aaronson, M., 1977, Ph.D. Thesis, Harvard University.
- Blietz, M., Cameron, M., Drapatz, S., Genzel, R., Krabbe, A., Van Der Werf, P., Sternberg, A., & Ward, M., 1994, Ap.J., 421, 92.
- Cardelli, J. A., Clayton, G. C., & Mathis, J. S., 1989, Ap.J., 345, 245.
- De Grijp, M. H. K., Keel, W. C., Miley, G. K., Goudfrooij, P., & Lub, J., 1992, A.&A.Supp., 96, 389.
- Eracleous, M., Livio, M., & Binette, L. 1995, Ap.J., in press.
- Fabbiano, G., Fassnacht, C., & Trinchieri, G., 1994, Ap.J., 434, 67.
- Filippenko, A. V., & Sargent, W. L. W. 1985, Ap.J.Supp., 57, 503.

- Ford, H. C., Dahari, O., Jacoby, G. H., Crane, P. C., & Ciardullo, R., 1986, *Ap.J.*, 311, L7.
- Graham, J. R., Wright, G. S., & Longmore, A. J., 1987, *Ap.J.*, 313, 847.
- Graham, J. R., Wright, G. S., & Longmore, A. J., 1990, *Ap.J.*, 352, 172.
- Graham, J. R., Wright, G. S., Hester, J. J., & Longmore, A. J., 1991, *A.J.*, 101, 175.
- Hall, D. N. B., 1973, *Kitt Peak National Observatory: An Atlas of Infrared Spectra of the Solar Photosphere and of Sunspot Umbrae*.
- Halpern, J. P., & Grindlay, J. E., 1980, *Ap.J.*, 242, 1041.
- Heckman, T. M., 1980, *A&A*, 87, 152.
- Heckman, T. M., Balick, B., & Crane, P. C., 1980, *A&A*, 40, 295.
- Ho, L. C., Filippenko, A. V., & Sargent, W. L. W., 1993, *Ap.J.*, 417, 63.
- Hoffleit, D., 1964, *Catalogue of Bright Stars, Yale University Observatory, Third Revised Edition*.
- Keel, W. C., 1983, *Ap.J.*, 269, 466.
- Larkin, J. E., Armus, L., Knop, R. A., Murphy, T. W., & Soifer, B. T., 1997, in preparation.
- Larkin, J. E., Knop, R. A., Lin, S., Matthews, K., & Soifer, B. T., 1996, *P.A.S.P.*, 108, 211.
- Maoz, D., Filippenko, A. V., Ho, L. C., Rix, H. W., Bahcall, J. N., Schneider, D. P., & Macchetto, F. D., 1995, *Ap.J.*, 440, 91.
- Mollenhoff, C., & Bender, R., 1989, *A&A*, 214, 61.
- Moorwood, A. F. M., & Oliva, E., 1988, *A&A*, 203, 278.
- Mouri, H., Taniguchi, Y., Kawara, K., & Nishida, M., 1989, *Ap.J.*, 346, L73.
- Mouri, H., & Taniguchi, Y., 1992, *Ap.J.*, 386, 68.
- Miyoshi, M., Moran, J., Herrnstein, J., Greenhill, L., Nakai, N., Diamond, P., & Inoue, M., *Nature*, 373, 127.
- Nakai, N., Inoue, M., & Miyoshi, M., 1993, *Nature*, 361, 45.
- Neugebauer, G., Elias, J., Matthews, K., McGill, J., Scoville, N., & Soifer, B. T., 1987, *A.J.*, 93, 1057.
- Nussbaumer, H., & Storey, P. J., 1988, *A&A*, 193, 327.
- Oliva, E., Moorwood, A. F. M., & Danziger, I. J., 1989, *A&A*, 214, 307.
- Oliva, E., & Origlia, L., 1992, *A&A*, 254, 466.
- Osterbrock, D. E., 1989, *Astrophysics of Gaseous Nebulae and Active Galactic Nuclei*, University Science Books.

- Seab, C. G., & Shull, J. M., 1983, *Ap.J.*, 275, 652.
- Serlemitsos, P., 1995, conference proceedings, *The Physics of LINERs in View of Recent Observations*, in preparation.
- Shields, J. C. 1992, 399, L27.
- Storchi-Bergmann, T., Baldwin, J. A., & Wilson, A. S., 1993, *Ap.J.*, 410, L11.
- Terlevich, R., & Melnick, J., 1985, *M.N.R.A.S.*, 213, 841.
- Van Der Werf, P. P., Genzel, R., Krabbe, A., Blietz, M., Lutz, D., Drapatz, S., Ward, M., J., & Forbes, D. A., 1993, *Ap.J.*, 405, 522.
- Willner, S. P., Elvis, M., Fabbiano, G., Lawrence, A., & Ward, M. J. 1985, *Ap.J.*, 299, 443.